EARTHQUAKE ENGINEERING AND STRUCTURAL DYNAMICS, VOL. 5, 107–129 (1977)

ANTIPLANE DYNAMIC SOIL-BRIDGE INTERACTION FOR INCIDENT PLANE SH-WAVES

A. M. ABDEL-GHAFFAR† AND M. D. TRIFUNAC‡

Department of Civil Engineering, California Institute of Technology, Pasadena, California, U.S.A.

SUMMARY

The analysis of dynamic soil-bridge interaction has been performed in three steps. These are:

1. The analysis of input motions.
2. The force-displacement relationships for the foundations.
3. The dynamic analysis of the structure itself, i.e. the bridge.

Based on the exact solution of the first two steps, the dynamic interaction of a simple two-dimensional bridge model erected on an elastic half-space has been investigated for a single span case. The two-dimensional model under study consists of an elastic shear girder bridge supported by two rigid abutments and rigid foundations which have a circular cross-section and are welded to the half-space. It has been shown that the dynamic interaction depends on:

1. The incidence angle of plane SH-waves.
2. The ratio of the rigidity of the girder and the soil.
3. The ratio of the girder mass to the mass of the rigid abutment-foundation system.
4. The span of the bridge.

The dynamic response of the girder and the effect of the radiative damping in the half-space on the interaction of the girder have been studied.

INTRODUCTION

The problem of the dynamic interaction between buildings and the soil during earthquake excitation has attracted the considerable interest of many investigators.[1–5] However, such analyses have, so far, not been extended to more complicated structures, such as bridges or large industrial buildings, where differential motions of foundations might influence response in an important way.

There have been many cases reported in the literature in which bridges suffered damage during earthquakes.[6,7] These examples clearly indicate the need for detailed investigations of the dynamic soil-bridge interaction to determine the significance of that interaction on the bridge response. The soil-bridge interaction effect is considered important, for example, when the motion of an abutment or foundation is significantly different from the motion of the ground in the absence of the bridge, the latter motion being usually referred to as the free-field ground motion.

The general dynamic soil-structure interaction problem can be broken down into three parts.[8] These are:

1. The determination of the input motion to the foundations (the contribution of the seismic waves) or equivalently the determination of the driving forces.

2. The evaluation of the force-displacement relationship (the impedance functions or their reciprocal, the compliance functions) for the foundations.

3. The solution of the equations of motion including both the foundations and the superstructure.

This approach has the advantage that once the solutions of the first two parts have been obtained for a class of foundations, the results can be used to calculate the interaction response of different structures. This is done by superimposing the results so that the equations of motion for the foundations are satisfied. This method, of course, is possible only if the problem is linear.

---

† Graduate Student.
‡ Formerly Assistant Professor, Division of Engineering and Applied Science. Present address: University of Southern California, University Park, Los Angeles, California, U.S.A.

Received 30 July 1975
Revised 6 January 1976

Luco and Contesse[5] have studied the dynamic interaction, through the soil for two parallel infinite shear walls placed on rigid foundations and for vertically incident SH-waves. In a similar study Wong and Trifunac[9] have determined the driving forces induced by harmonic plane SH-waves and the impedance functions for a class of embedded foundations with circular cross sections at different separation distances. We will use these results in the present analysis of a two-dimensional superstructure (the girder), the substructure (the two abutments) and the two foundations.

The model considered in this paper offers obvious analytical advantages and a simple and direct insight into a complicated wave propagation phenomenon. However, this model represents a highly simplified version of actual three-dimensional problem, in which in-plane as well as anti-plane incident waves are present and where coupling between the horizontal, rocking, torsional and vertical motions of the structure and the foundations take place.

THE MODEL, THE EXCITATION AND THE EXACT SOLUTION

The two-dimensional model studied in this paper is shown in Figure 1(a). It consists of three structural elements: the superstructure (the girder), the substructure (the abutments) and the foundations. These

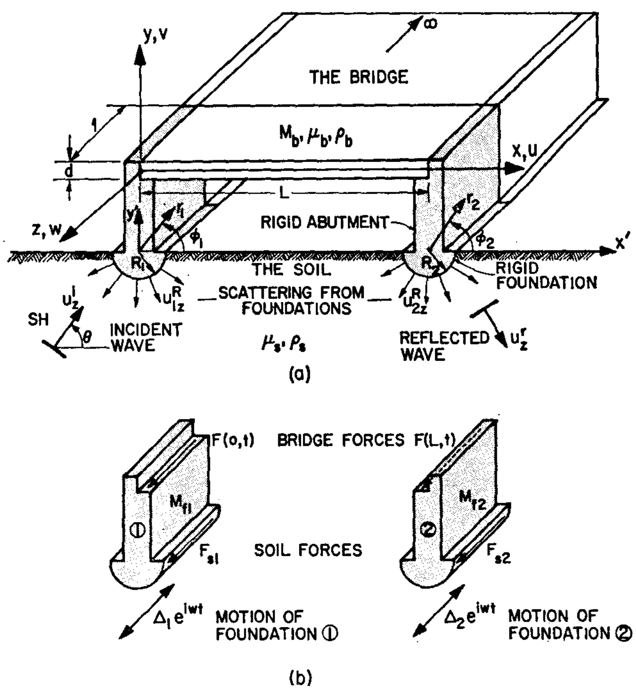

Figure 1. (a) Bridge, two foundations and the co-ordinate systems, (b) forces acting on the two rigid foundations

elements are assumed to be infinitely extended in the z-direction. Furthermore, the following assumptions are made:

1. The soil, which is represented by the half-space, is elastic, isotropic and homogeneous. Its rigidity and the velocity of shear waves are μ_s and β_s, respectively.
2. The two foundations are assumed to be rigid, semicircular in cross-section and welded to the half-space.
3. The abutments are also assumed to be rigid. They are welded to the foundations so they behave together as a rigid body partially embedded in the soil.
4. The model for the girder is a shear beam, of span L and depth d, supported at the ends by the rigid piers. The beam is isotropic and homogeneous; the rigidity and the velocity of the shear waves in the beam are given by μ_b and β_b, respectively.

The co-ordinate systems

1. For the superstructure, i.e. the girder, the origin of x and y co-ordinates is located at the left support point as shown in Figure 1(a). The x-axis is defined along the span of the bridge, while the y-axis is in the vertical direction.

2. For the two rigid abutment-foundation systems, the scattered waves from the two rigid foundations are best represented by polar co-ordinates (r_1, ϕ_1) and (r_2, ϕ_2), which have their origins at the centre of each foundation. The cartesian co-ordinates (x', y') are located at the left foundation such that

$$\left\{\begin{matrix} x_1 \\ x_2 \end{matrix}\right\} = \left\{\begin{matrix} x' \\ x'-L \end{matrix}\right\} = \left\{\begin{matrix} r_1 \cos\phi_1 \\ r_2 \cos\phi_2 \end{matrix}\right\}, \quad \left\{\begin{matrix} y_1 \\ y_2 \end{matrix}\right\} = \left\{\begin{matrix} r_1 \sin\phi_1 \\ r_2 \sin\phi_2 \end{matrix}\right\} \tag{1}$$

This choice of the (r_1, ϕ_1) and (r_2, ϕ_2) co-ordinate systems is identical to that used by Wong and Trifunac.[9]

As shown by several investigators,[5,9,10] the interaction problem can be separated into three steps:

(i) Input motion or 'driving forces'.

(ii) Impedance functions or 'compliance functions'.

(iii) Dyanmic analysis of the structure (bridge).

The final results are then obtained by superposition. Some parts of these analyses are given in this paper for the completeness of this presentation, as follows:

I. MOTION OF THE SOIL

We assume that the excitation is in the form of plane harmonic SH-waves with an amplitude equal to one and with the angle of incidence θ, which is measured counterclockwise from the horizontal axis to the normal on the plane wave front [Figure 1(a)]. This incident wave is given by

$$u_z^i(x', y', t) = \exp\left[i\omega(t - x'/c_x - y'/c_y)\right] \tag{2}$$

where

$$c_x = \frac{\beta_s}{\cos\theta}, \quad c_y = \frac{\beta_s}{\sin\theta} \tag{3}$$

and $\beta_s = \sqrt{(\mu_s/\rho_s)} \ldots$ is the shear wave velocity in the soil, μ_s is the shear modulus of the soil and ρ_s is the density.

The resulting free-field motion, i.e. motion of the half-space in the absence of the bridge and its foundations, becomes

$$u_z^{i+r}(x', y', t) = 2\exp\left\{i\omega t\left[\exp\left(-i\frac{\omega}{\beta_s}x'\cos\theta\right)\right]\right\}\cos\left(\frac{\omega y'}{\beta_s}\sin\theta\right) \tag{4}$$

where u_z^{i+r} stands for the sum of incident, u_z^i, and reflected, u_z^r, waves from the half space boundary $y' = 0$. This motion can be represented in terms of polar co-ordinates (r_1, ϕ_1) and (r_2, ϕ_2).[9]

The total displacement field, u_z, in the half-space in the presence of the two rigid foundations is composed of the free-field motion u_z^{i+r} and the scattered waves, u_{1z}^R and u_{2z}^R, from the two foundations, i.e.

$$u_z = u_z^{i+r} + u_{1z}^R + u_{2z}^R \tag{5}$$

This total displacement, u_z, must satisfy the Helmholtz equation in each of the (r_1, ϕ_1) and (r_2, ϕ_2) co-ordinate systems

$$\frac{\partial^2 u_z}{\partial r_j^2} + \frac{1}{r_j}\frac{\partial u_z}{\partial r_j} + \frac{1}{r_j^2}\frac{\partial^2 u_z}{\partial \phi_j^2} + k_s^2 u_z = 0, \quad j = 1, 2 \tag{6}$$

in which $k_s = \omega/\beta_s$ is the wave number, and the two boundary conditions

(i) Stress-free surface boundary condition

$$\sigma_{\phi_j z} = \frac{\mu_s}{r_j}\frac{\partial u_z}{\partial \phi_j} = 0 \quad \text{at } \phi_j = -\pi, 0, \; j = 1, 2, \quad r_j \geqslant R_j \tag{7}$$

(ii) Harmonic displacement boundary condition

$$u_z(R_j, \phi_j, t) = \Delta_j \exp(i\omega t), \quad -\pi \leqslant \phi_j \leqslant 0, \quad j = 1, 2 \tag{8}$$

where Δ_1 and Δ_2 are the displacement amplitudes of the two foundations [Figure 1(b)]. Δ_1 and Δ_2 are unknown and depend on the soil-structure interaction of both foundations and the characteristics of the incoming waves.

The three cases which are superposed in the analysis of this interaction problem are illustrated in Figure 2(a). This figure represents a generalization of the solution method presented by Wong and Trifunac[9] to the soil-bridge interaction problem studied in this paper.

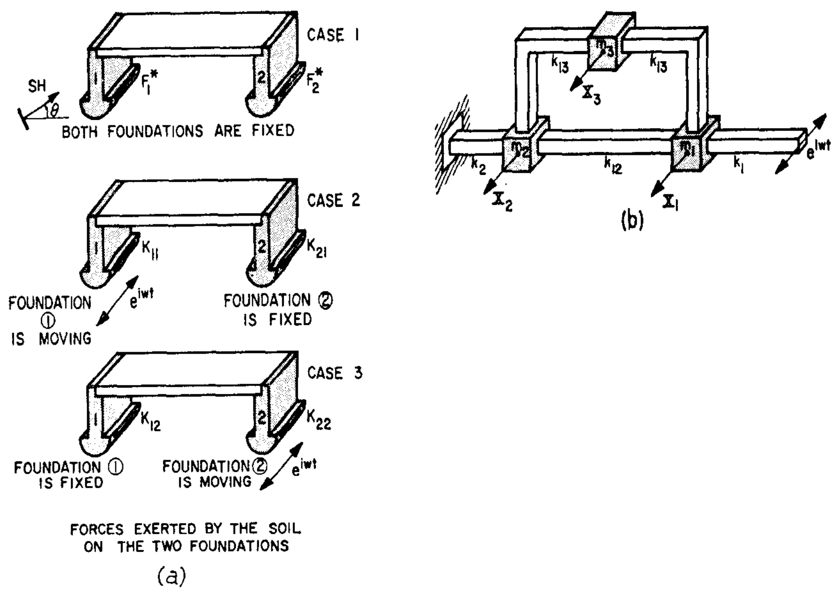

Figure 2. (a) Forces exerted by the soil on the two foundations, (b) a simplified discrete model

II. FORCES GENERATED BY THE SOIL AND COMPLIANCE FUNCTIONS

The forces exerted by the soil on the two foundations and caused by the incident waves and the motion of the neighbouring foundations, as shown in Figure 1(b), are given by

$$\begin{Bmatrix} F_{s1} \\ \\ F_{s2} \end{Bmatrix} = - \begin{Bmatrix} -\int_{-\pi}^{0} \sigma_{rz}(R_1, \phi_1)\, R_1\, \mathrm{d}\phi_1 \\ \\ -\int_{-\pi}^{0} \sigma_{rz}(R_2, \phi_2)\, R_2\, \mathrm{d}\phi_2 \end{Bmatrix} \tag{9}$$

where

$$\sigma_{rz}(R_i, \phi_i) = \mu_s \left.\frac{\partial u_z}{\partial r_i}\right|_{r_i = R_i}, \quad i = 1, 2 \tag{10}$$

Using the principle of superposition, the total soil forces can be expressed in terms of the 'driving forces', and the unknown displacements $\{\Delta\}$ premultiplied by the impedance matrix,

$$\begin{Bmatrix} F_{s1} \\ F_{s2} \end{Bmatrix} = \begin{Bmatrix} -F_1^* \\ -F_2^* \end{Bmatrix} + \begin{bmatrix} K_{11} & K_{12} \\ K_{21} & K_{22} \end{bmatrix} \begin{Bmatrix} \Delta_1 \\ \Delta_2 \end{Bmatrix} \tag{11}$$

Here the driving forces F_1^* and F_2^* are the forces exerted by the soil on the two foundations which are held fixed during excitation by the incident waves u_z^i. The driving forces depend on the properties of the foundations and the soil and also on the nature of the seismic excitation. An element of the impedance matrix

K_{ij} $(i, j = 1, 2)$ represents the force acting on the motionless ith foundation caused by the unit harmonic motion of the jth foundation. The impedance matrix depends only on the characteristics of the foundations and soil and on the frequency of the motion. Figure 2(a) illustrates the physical meaning of these force coefficients.

III. DYNAMIC ANALYSIS OF THE BRIDGE

A. Motion of the bridge

The displacements u and v of the two-dimensional bridge model are selected to be zero, while the displacement w depends only on the co-ordinate x. This displacement must satisfy the equation of motion of an undamped shear beam

$$\frac{\partial^2 w(x,t)}{\partial x^2} = \frac{1}{\beta_b^2}\frac{\partial^2 w(x,t)}{\partial t^2}, \quad 0 \leqslant x \leqslant L \tag{12}$$

in which $\beta_b = \sqrt{(\mu_b/\rho_b)}$ ... is the shear wave velocity in the beam, μ_b is the shear modulus of the beam and ρ_b is the density of the beam.

The boundary conditions for the beam are

$$\begin{Bmatrix} w(0,t) \\ w(L,t) \end{Bmatrix} = \begin{Bmatrix} \Delta_1 \\ \Delta_2 \end{Bmatrix} \exp(i\omega t) \tag{13}$$

where Δ_1 and Δ_2 are the unknown complex displacements of the two foundations. The solution of equation (12), compatible with the boundary conditions given by equation (13), is

$$w(x,t) = \{[\cos(k_b x) - \cot(k_b L)\sin(k_b x)],\ [\operatorname{cosec}(k_b L)\sin(k_b x)]\}\begin{Bmatrix} \Delta_1 \\ \Delta_2 \end{Bmatrix}\exp(i\omega t) \tag{14}$$

in which $k_b = \omega/\beta_b$ ... is the wave number in the shear beam. From equation (14) it is seen that the displacement $w(x,t)$ depends on the instantaneous values of the harmonic boundary conditions.

B. Forces exerted by the bridge

The end resisting forces, per unit length, acting on the two abutments [Figure 1(b)] are given by

$$\begin{Bmatrix} F_1^b(t) \\ F_2^b(t) \end{Bmatrix} = \begin{Bmatrix} F(0,t) \\ F(L,t) \end{Bmatrix} = \begin{Bmatrix} d\sigma_{xz}^b(0,t) \\ -d\sigma_{xz}^b(L,t) \end{Bmatrix} = \begin{Bmatrix} -\mu_b d\dfrac{\partial w(0,t)}{\partial x} \\ -\mu_b d\dfrac{\partial w(L,t)}{\partial x} \end{Bmatrix} \tag{15}$$

where d is the depth of the shear beam and σ_{xz}^b is the shear stress in the z-direction.

By using equations (14) and (15), and by introducing the expression

$$M_b = \rho_b dL \tag{16}$$

which corresponds to the mass of the beam per unit length in the z-direction, these support forces can be written as

$$\begin{Bmatrix} F_1^b(t) \\ F_2^b(t) \end{Bmatrix} = \begin{bmatrix} -\omega^2 M_b \dfrac{\cot(k_b L)}{(k_b L)} & \omega^2 M_b \dfrac{\operatorname{cosec}(k_b L)}{(k_b L)} \\ \omega^2 M_b \dfrac{\operatorname{cosec}(k_b L)}{(k_b L)} & -\omega^2 M_b \dfrac{\cot(k_b L)}{(k_b L)} \end{bmatrix} \begin{Bmatrix} \Delta_1 \\ \Delta_2 \end{Bmatrix} \exp(i\omega t) \tag{17}$$

It is convenient to recall here that the undamped natural frequencies of the simply supported shear beam are given by

$$\omega_n = \frac{n\pi}{L}\sqrt{\left(\frac{\mu_b}{\rho_b}\right)} = \frac{n\pi}{L}\beta_b, \quad n = 1,2,3,\ldots \tag{18}$$

This corresponds to

$$k_b L = n\pi, \quad n = 1,2,3,\ldots. \tag{19}$$

The mode shapes are given by

$$W_n(x) = \sin\frac{n\pi x}{L}, \quad n = 1,2,3,\ldots \tag{20}$$

Dynamic soil-bridge-soil interaction

The unknown foundation displacement amplitudes Δ_1 and Δ_2 can now be determined from the balance of forces exerted on each foundation. These forces are

1. Soil forces F_{s1} and F_{s2}, as given by equation (11).
2. Bridge end forces $F_1^b(t)$ and $F_2^b(t)$, as given by equation (17).
3. Inertia forces of each rigid abutment-foundation system, with masses M_{f1} and M_{f2}, and accelerations $-\omega^2\Delta_1\exp(i\omega t)$ and $-\omega^2\Delta_2\exp(i\omega t)$, as shown in Figure 1(b).

The balance of the forces for the two abutment-foundation systems is then

$$\left.\begin{aligned} -\omega^2\Delta_1 M_{f1} &= -[-F_1^* + K_{11}\Delta_1 + K_{12}\Delta_2 + F_1^b(t)] \\ -\omega^2\Delta_2 M_{f2} &= -[-F_2^* + K_{21}\Delta_1 + K_{22}\Delta_2 + F_2^b(t)] \end{aligned}\right\} \tag{21}$$

Introducing

$$\begin{Bmatrix} M_{s1} \\ M_{s2} \end{Bmatrix} = \frac{\pi}{2}\rho_s \begin{Bmatrix} R_1^2 \\ R_2^2 \end{Bmatrix} \tag{22}$$

which corresponds to the mass of the soil per unit length removed by the two foundations and by using equations (17) and (21) there follows

$$\begin{bmatrix} \left[\frac{k_s R_1}{2}\left(\frac{M_{f1}}{M_{s1}} + \frac{M_b}{M_{s1}}\frac{\cot(k_b L)}{(k_b L)}\right) - \bar{K}_{11}\right] & \left[-\frac{k_s R_1}{2}\left(\frac{M_b}{M_{s1}}\frac{\operatorname{cosec}(k_b L)}{(k_b L)}\right) - \bar{K}_{12}\right] \\ \left[-\frac{k_s R_2}{2}\left(\frac{M_b}{M_{s2}}\frac{\operatorname{cosec}(k_b L)}{(k_b L)}\right) - \bar{K}_{21}\right] & \left[\frac{k_s R_2}{2}\left(\frac{M_{f2}}{M_{s2}} + \frac{M_b}{M_{s2}}\frac{\cot(k_b L)}{(k_b L)}\right) - \bar{K}_{22}\right] \end{bmatrix} \begin{Bmatrix} \Delta_1 \\ \Delta_2 \end{Bmatrix} = \begin{Bmatrix} \bar{F}_1^* \\ \bar{F}_2^* \end{Bmatrix} \tag{23}$$

where

$$\begin{Bmatrix} K_{11} \\ K_{12} \end{Bmatrix} = \mu_s \pi k_s R_1 \begin{Bmatrix} \bar{K}_{11} \\ \bar{K}_{12} \end{Bmatrix}, \quad \begin{Bmatrix} K_{21} \\ K_{22} \end{Bmatrix} = \mu_s \pi k_s R_2 \begin{Bmatrix} \bar{K}_{21} \\ \bar{K}_{22} \end{Bmatrix}$$

and

$$\begin{Bmatrix} F_1^* \\ F_2^* \end{Bmatrix} = \mu_s \pi k_s \begin{Bmatrix} R_1 \bar{F}_1^* \\ R_2 \bar{F}_2^* \end{Bmatrix} \tag{24}$$

The foundation displacement amplitudes Δ_1 and Δ_2 are uniquely determined by solving the two simultaneous, complex and non-homogeneous equations (23).

Numerical examples presented in Figures 3 to 12 depend mainly on the angle of incident waves θ and five other dimensionless parameters.

1. $\eta = (\omega/\beta_s) R_1 = k_s R_1 = (2\pi/\lambda_s) R_1$, which is the dimensionless frequency which compares the wavelength λ_s of the incident wave to the width of the left foundation.

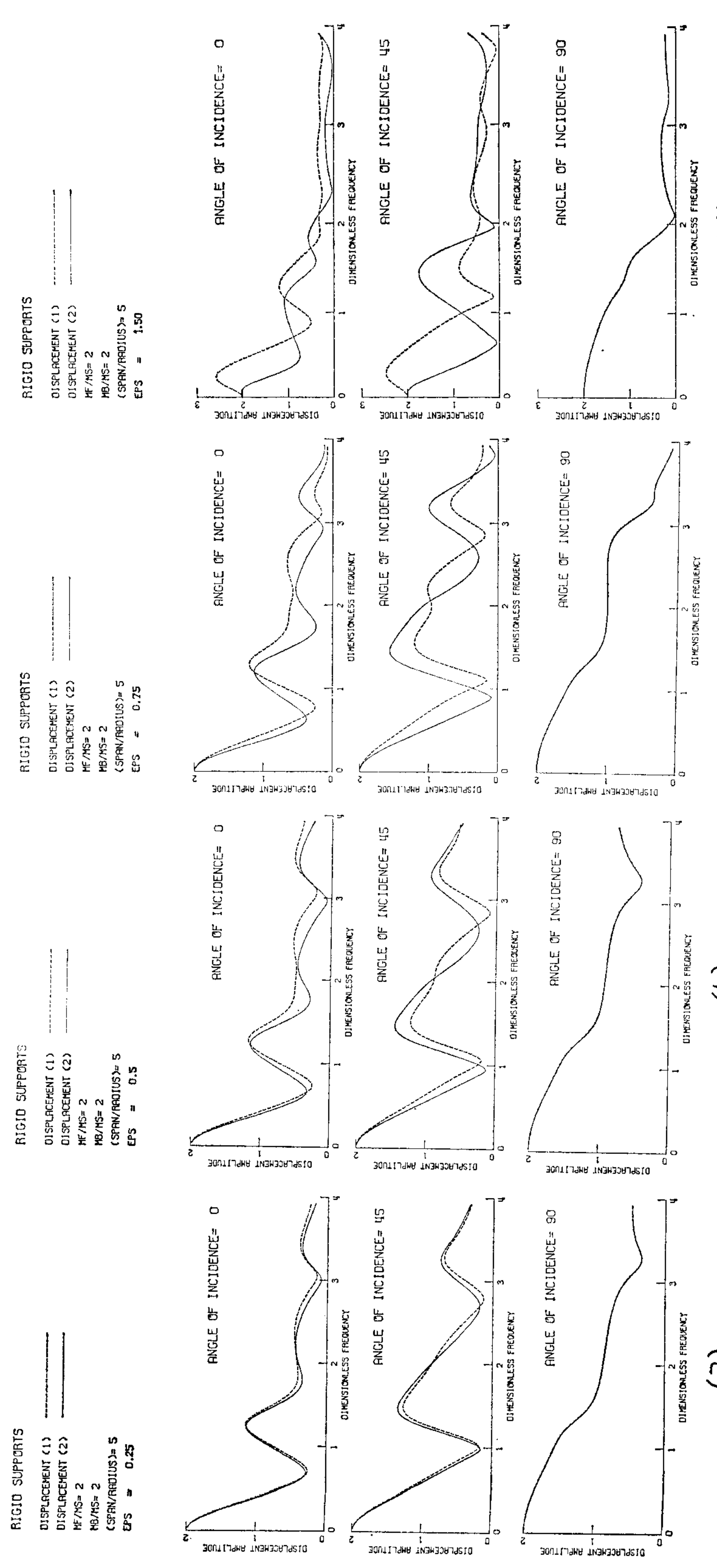

Figure 3. Foundation displacements Δ_1 and Δ_2 for MF/MS = 2, MB/MS = 2, $R_1 = R_2$, $L/R_2 = 5$ and $\varepsilon = 0{\cdot}25$, $0{\cdot}5$, $0{\cdot}75$ and $1{\cdot}5$

2. M_{f1}/M_{s1} and M_{f2}/M_{s2}, which are the ratios of the masses of the abutment-foundation systems to the masses of the soil replaced by the foundation only. They are set equal in the examples considered in this paper (i.e. $M_{f1}/M_{s1} = M_{f2}/M_{s2} = \mathrm{MF/MS}$).

3. M_b/M_{s1} and M_b/M_{s2}, which are the ratios of the mass of the bridge girder to the masses of the soil replaced by its foundations. (In the figures these are denoted by MB/MS when $R_1 = R_2$ and by MB/MS1 and MB/MS2 when $R_1 \neq R_2$.)

4.

$$\varepsilon = \frac{k_b L}{k_s R_2} = \frac{\beta_s}{\beta_b}\frac{L}{R_2} = \frac{\beta_s}{\beta_b}\frac{L}{R_1}\frac{R_1}{R_2}$$

this ratio reflects the relative stiffness of the bridge and the soil; it also describes the ratio of the span to the radius of the foundation. Large values of ε indicate a more flexible bridge with respect to the soil and/or a longer span, while $\varepsilon = 0$ implies a rigid structure composed of a rigid bridge girder, rigid abutments and rigid foundations. In that case $\Delta_1 = \Delta_2$.

5. R_1/R_2; this geometric parameter which reflects the relative width of the two foundations is also needed unless $R_1 = R_2$. For different types of soil and a typical reinforced concrete structure 'bridge' with μ, γ and β as shown in Table I and for selected ratios of L/R_2 and R_1/R_2, the range of values for ε is as shown in Table II.

Table I. Typical values of μ, γ and β for reinforced concrete girder bridge and different 'soils'

Property	Superstructure R.C. girder bridge	Different soils I	II	III	IV
μ, K/ft^2	288,000	1,400	5,130	15,530	388,200
γ, K/ft^3	0·15	0·125	0·125	0·125	0·125
β, ft/s	7,000	600	1,150	2,000	10,000
β_b/β_s		13·17	6·87	3·95	0·79

Table II. The range of values for ϵ

	Different soils I	II	III	IV	L/R_2	R_1/R_2
$\epsilon = \frac{k_b L}{k_s R_2} = \frac{\beta_s}{\beta_b}\frac{L}{R_2}$	0·39	0·73	1·27	6·33	5	1
	0·78	1·46	2·54	12·66	10	1
	1·17	2·19	3·81	18·99	15	1
	0·20	0·37	0·64	3·27	5	2
	0·39	0·73	1·27	6·33	10	2
	0·59	1·10	1·91	9·80	15	2
	0·13	0·24	0·42	2·11	5	3
	0·25	0·46	0·84	4·22	10	3
	0·38	0·73	1·26	6·33	15	3

μ = shear modulus. γ = weight per unit volume. β = shear wave speed, β_b for the bridge and β_s for the soil.

INTERPRETATION OF THE INTERACTION

The two displacement amplitudes Δ_1 and Δ_2 computed for the excitation corresponding to the incident plane harmonic SH-waves have been illustrated in Figures 3 to 12. The displacement of the left foundation Δ_1 is represented by a dashed line, and the displacement of the right foundation Δ_2 by a solid line. These two displacement amplitudes have been plotted against the dimensionless frequency η.

Different cases have been considered which correspond to the following parameters.

1. The mass ratios have been considered for four cases

a. $\frac{MF}{MS} = 2, \quad \frac{MB}{MS} = 2$

b. $\frac{MF}{MS} = 4, \quad \frac{MB}{MS} = 2$

c. $\frac{MF}{MS} = 2, \quad \frac{MB}{MS} = 4$

d. $\frac{MF}{MS} = 2, \quad \frac{MB}{MS2} = 2, \quad \frac{MB}{MS1} = 8$

2. The following geometric size ratios were examined: $L/R_2 = 5, 10$, for $R_1/R_2 = 1, 2$, respectively.

3. The relative stiffness ratio of the bridge girder and the soil, which is represented by the parameter ε (note: ε is written as EPS in these graphs), has been assumed to have the values 1, 2, 3 and 4.

4. The angle of incidence, θ, of plane SH-waves has taken the values equal to 0, 45, 90, 135 and 180 degrees. (Note: In the case of $R_1 = R_2$, we show only 0, 45 and 90 degrees because of symmetry.)

The figures have been arranged so that the influence of the angle of incidence and the relative stiffness ratio can be studied for the mass ratios and the geometric size ratios fixed in each figure. Each of these figures consists of parts (a), (b), (c) and (d) which correspond to different values of ε.

Some of the most important phenomena of the interaction of the bridge and the soil which may be noted in these results are as follows.

1. As $\varepsilon \to 0$, $\Delta_1 \to \Delta_2$ [from equation (23)]. In that case, we have a rigid structure composed of three elements (two foundations, two abutments and a girder) all acting as a rigid body. Figure 3(a) illustrates this case for ε small. When ε increases, the differences between Δ_1 and Δ_2 become more apparent. We note, however, that in all cases these amplitudes approach the low frequency limit of $|\Delta_1| = |\Delta_2| = 2$, which corresponds to the displacement amplitude of the surface of the half-space for incident SH-waves with unit amplitude.

The amplitude Δ_1 may become larger than Δ_2 due to the amplification effect caused by the scattering from the right foundation. In the cases of $\varepsilon = 1{\cdot}5$ in Figure 3(d), for example, or for $\varepsilon = 2{\cdot}0$ in Figures 4(b) and 5(b), the peaks of Δ_1 are considerably larger than 2 for small dimensionless frequencies.

2. In the case of $\theta = 90$ degrees, when $R_1 = R_2$, the two foundations are in phase and have the same amplitude. These amplitudes become zero when the beam is excited at its odd frequencies, i.e. the symmetric mode shapes. In that case

$$\eta = n\pi/\epsilon, \quad n = 1, 3, 5, \ldots \tag{25}$$

and the symmetric modes of the bridge are

$$W_n(x) = \sin n\pi x/L, \quad n = 1, 3, 5, \ldots \tag{26}$$

Thus, when $\theta = 90$ degrees and $R_1 = R_2$, the symmetry of vibration reduces mathematically to a single foundation problem.[2,3] When incident waves have a frequency corresponding to a fixed base frequency of this structure, the foundation(s) is(are) located at a node of the standing wave pattern and the structure above and the soil below are moving 180 degrees out of phase.

3. The dip of the displacement amplitude curve Δ_2, which occurs for a shallow angle of incidence $\theta = 0$, 45 degrees, is displaced towards the lower values of the dimensionless frequency η, as the flexibility of the bridge increases (Figures 4 and 7). If we compare Figues 4 and 6 and 7 and 9, we note that, for the same ε and the same L/R_2, as the mass of the bridge increases, the dip moves again towards low values of η, i.e. the frequency decreases.

This behaviour can be explained qualitatively by the simplified model consisting of three masses and several springs [shown in Figure 2(b)], where the spring constants k_1, k_2 and k_{12} depend upon the soil properties,

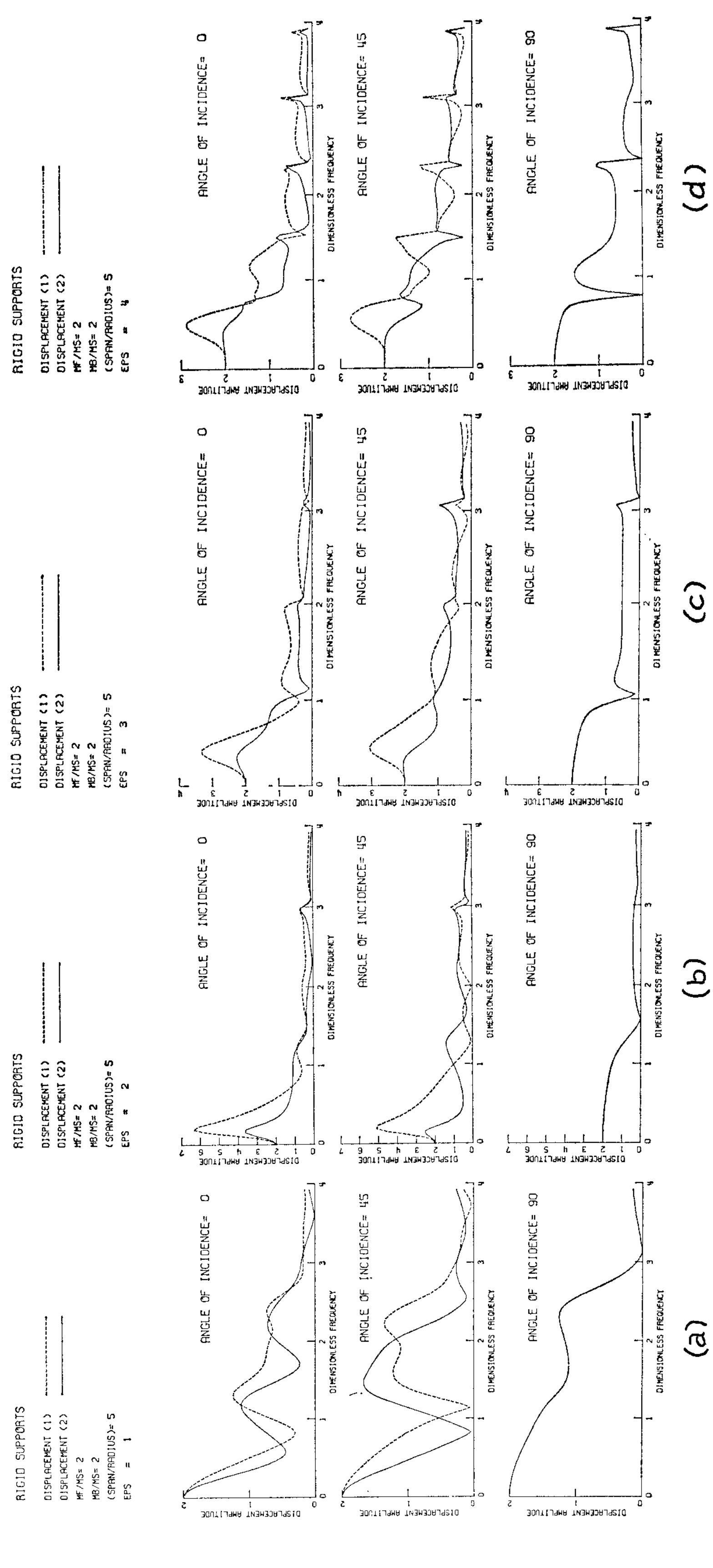

Figure 4. MF/MS = 2, MB/MS = 2, $R_1 = R_2$, $L/R_2 = 5$ and $\varepsilon = 1, 2, 3, 4$

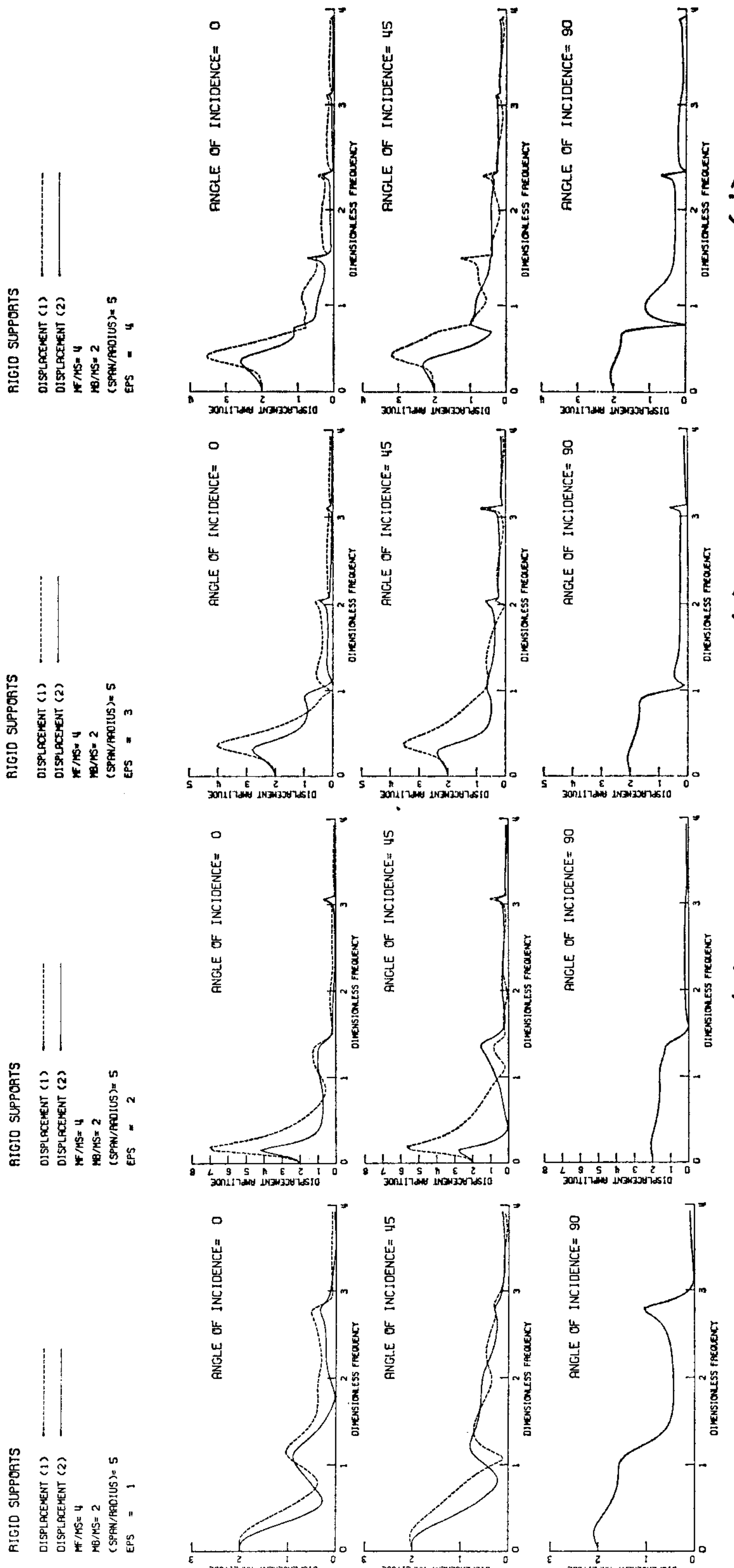

Figure 5. MF/MS = 4, MB/MS = 2, $R_1 = R_2$, $L/R_2 = 5$ and $\varepsilon = 1, 2, 3, 4$

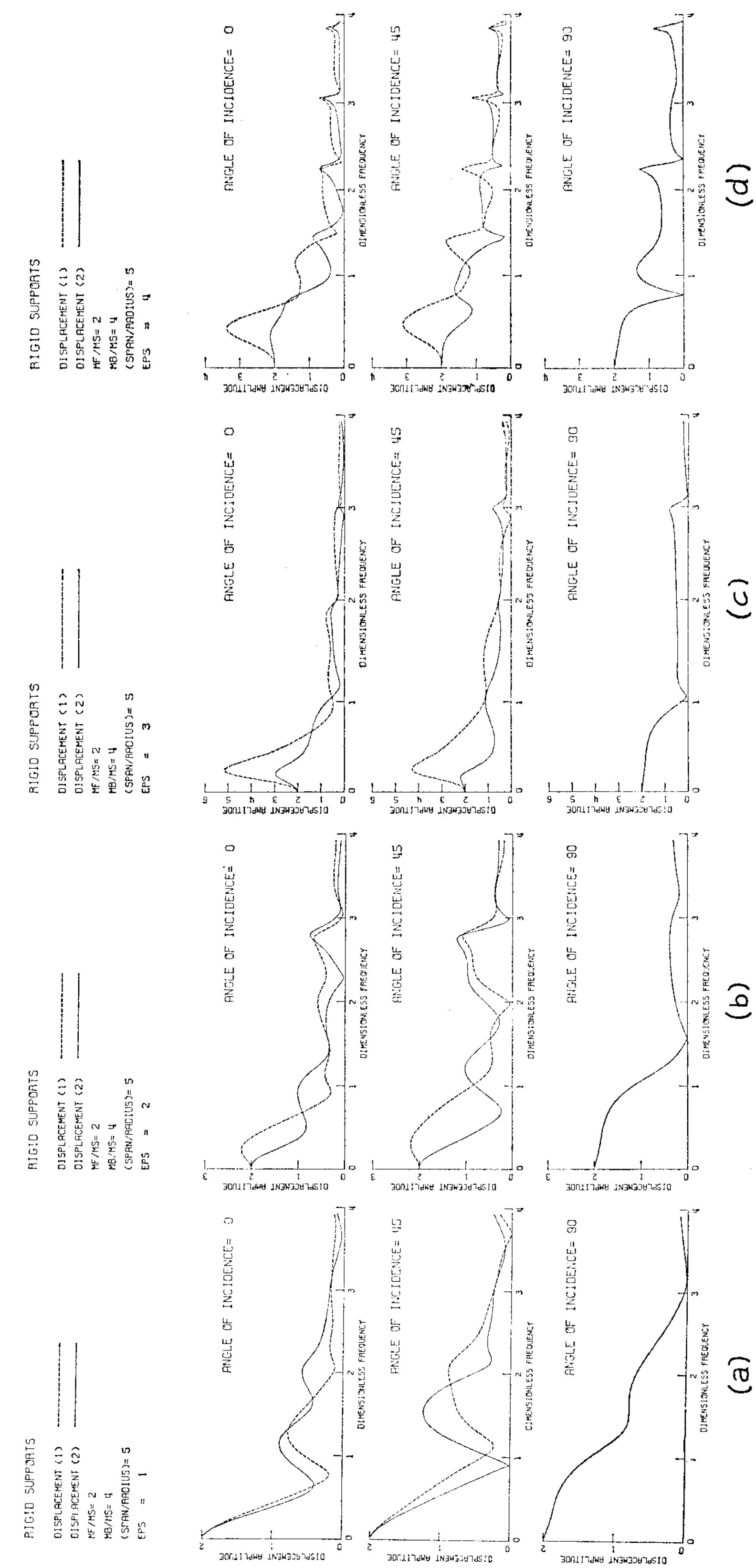

Figure 6. MF/MS = 2, MB/MS = 4, $R_1 = R_2$, $L/R_2 = 5$ and $\varepsilon = 1, 2, 3, 4$

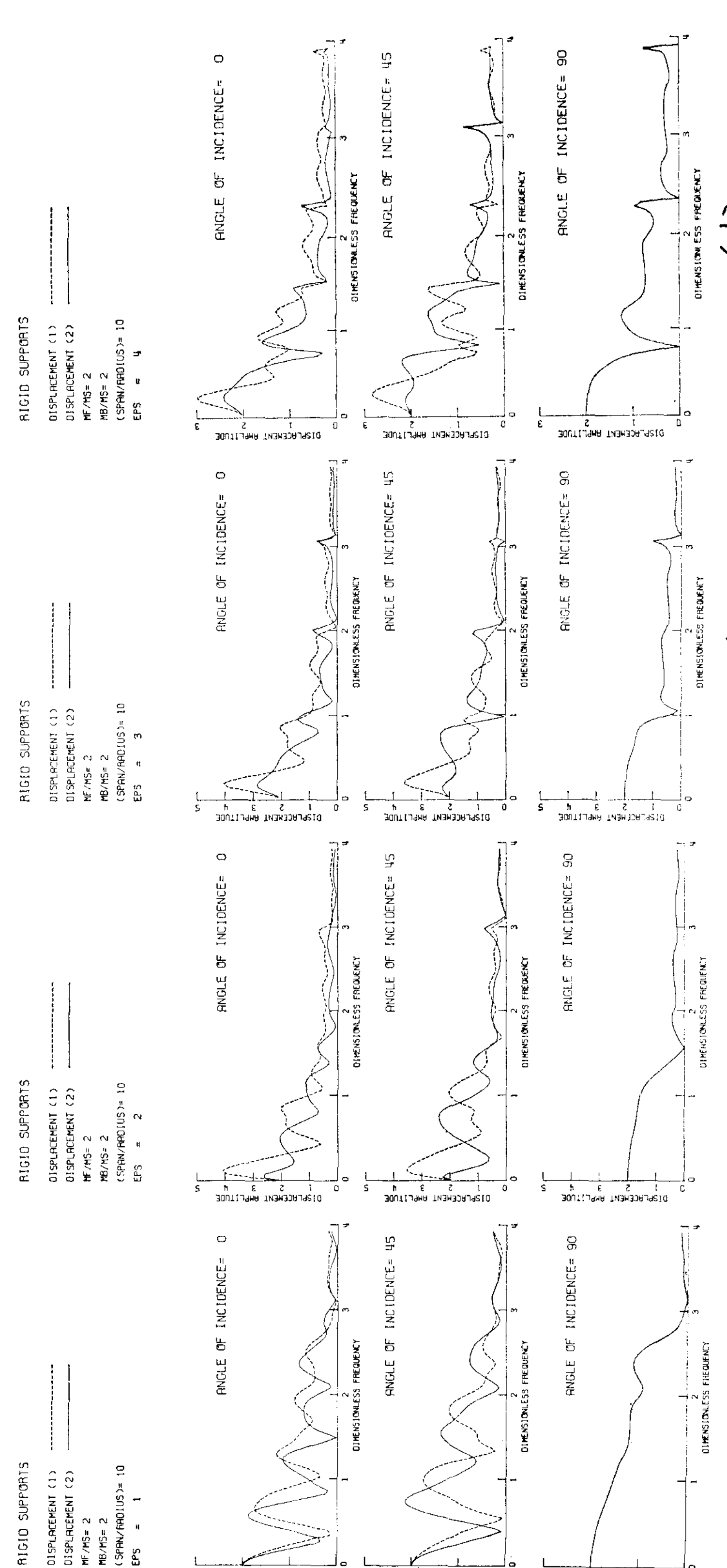

Figure 7. MF/MS = 2, MB/MS = 2, $R_1 = R_2$, $L/R_2 = 10$ and $\varepsilon = 1, 2, 3, 4$

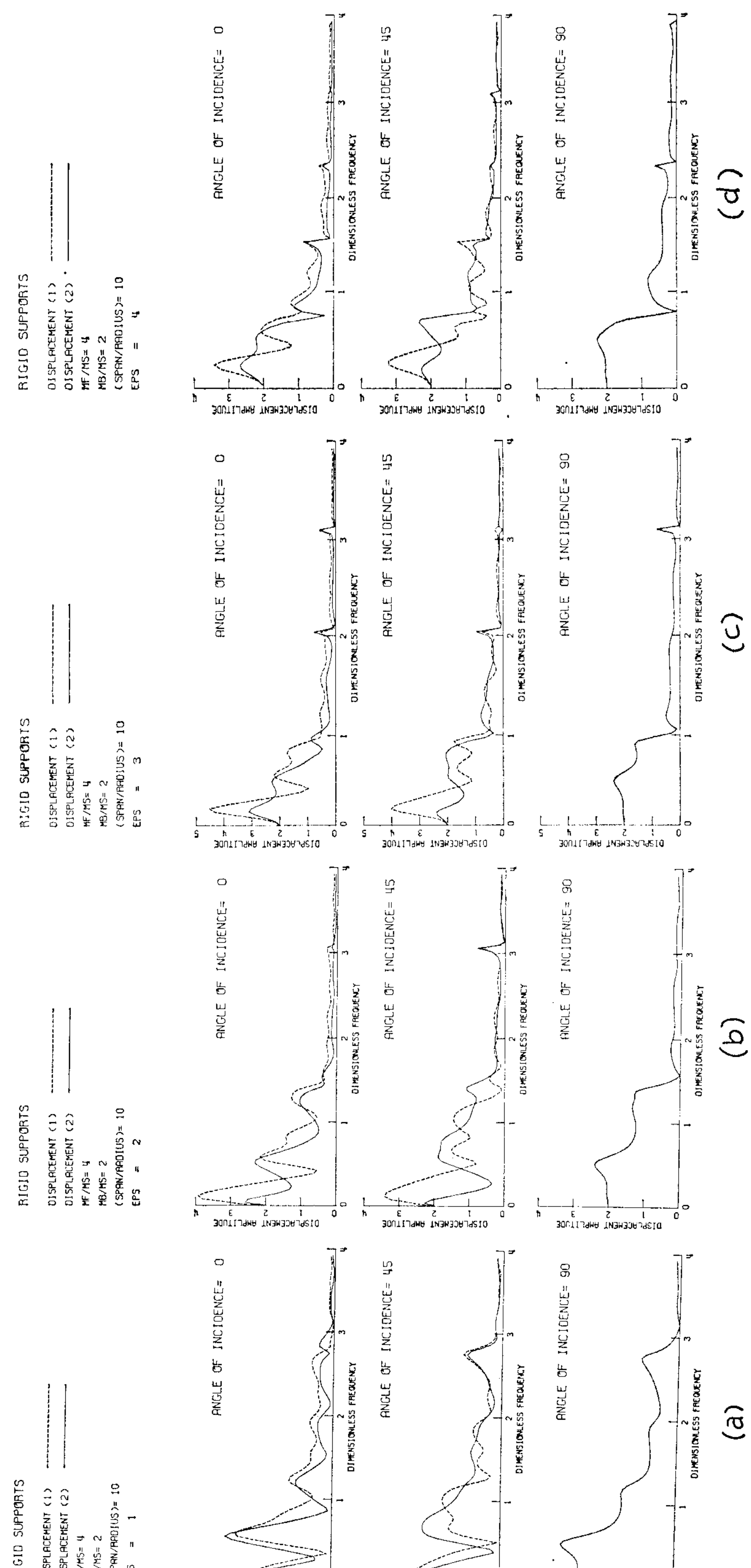

Figure 8. MF/MS = 4, MB/MS = 2, $R_1 = R_2$, $L/R_2 = 10$ and $\varepsilon = 1, 2, 3, 4$

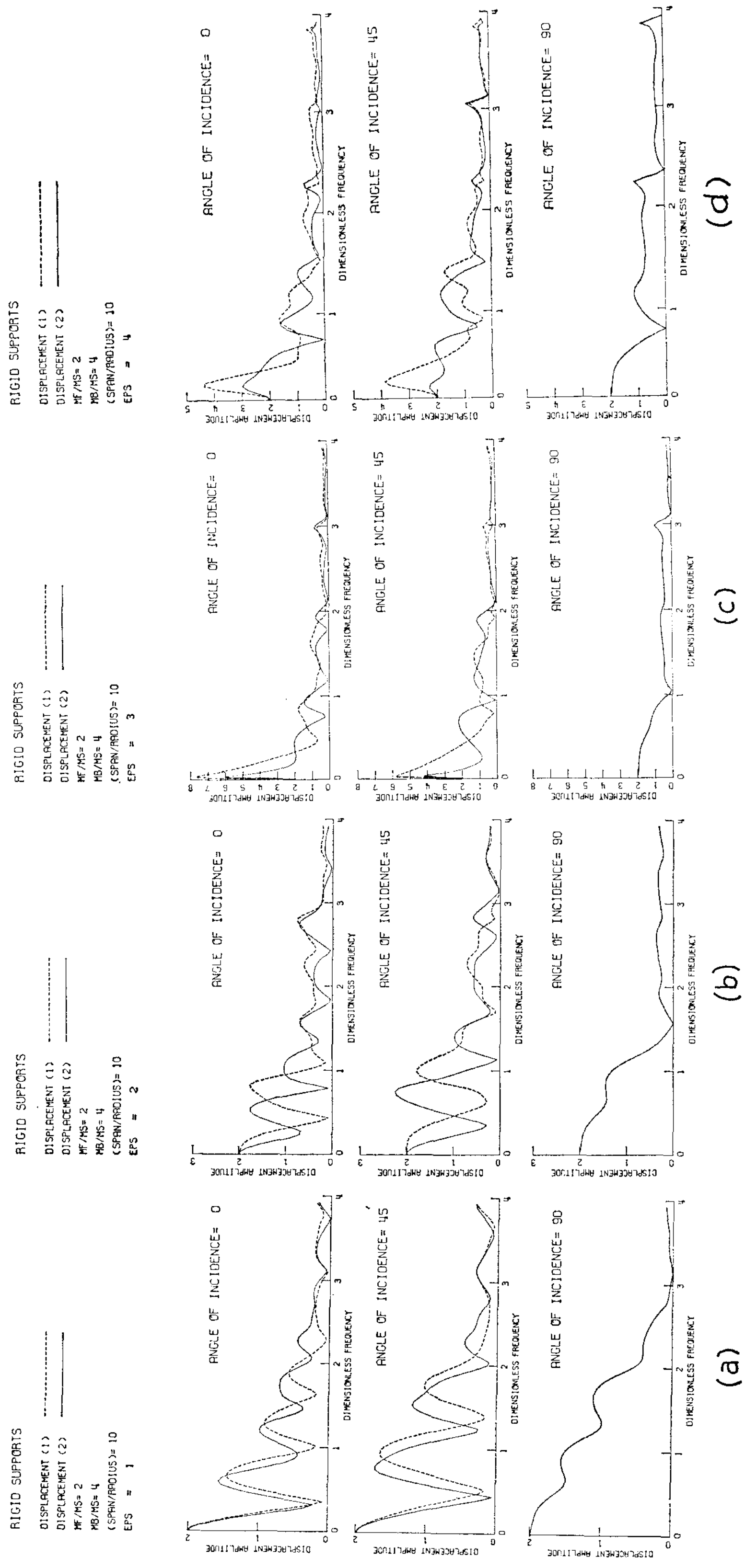

Figure 9. MF/MS = 2, MB/MS = 4, $R_1 = R_2$, $L/R_2 = 10$ and $\varepsilon = 1, 2, 3, 4$

while the spring constant k_{13} depends on the bridge stiffness. The displacements resulting from simple excitation, shown in Figure 2(b), can be determined from the following matrix equation

$$\begin{bmatrix} -\omega^2 m_1+k_1+k_{13}+k_{12} & -k_{12} & -k_{13} \\ -k_{12} & -\omega^2 m_2+k_2+k_{13}+k_2 & -k_{13} \\ -k_{13} & -k_{13} & -\omega^2 m_3+2k_{13} \end{bmatrix} \begin{Bmatrix} X_1 \\ X_2 \\ X_3 \end{Bmatrix} = \begin{Bmatrix} k_1 \\ 0 \\ 0 \end{Bmatrix} \tag{27}$$

where X_1, X_2 and X_3 are the displacement amplitudes of the three masses. $X_2 = 0$ when

$$k_{12}(-\omega^2 m_3+2k_{13})+k_{13}^2 = 0$$

i.e.

$$\omega_* = \sqrt{\left[\frac{k_{13}(2+k_{13}/k_{12})}{m_3}\right]} \tag{28}$$

This frequency depends on the absolute stiffness of the bridge k_{13} and the ratio of stiffness of the bridge with respect to the soil underneath it k_{13}/k_{12}. As the stiffness of the bridge k_{13} or the stiffness ratio k_{13}/k_{12} decrease, the frequency for which the dip occurs decreases (e.g. Figures 4, 6, 7 and 9). This frequency also decreases when the mass of the bridge increases. The above model is, of course, only a simple one-dimensional analogue, while our problem is a two-dimensional one involving propagation, reflection and scattering of waves from the rigid foundations in the soil and inside the beam. Nevertheless, in spite of its one-dimensional simplicity, the above model does allow one to obtain an approximate physical understanding of a more complicated wave propagation problem.

4. In all cases which have been shown in the figures for the non-vertical incidence of waves and when $\eta = n\pi/\varepsilon$, $n = 1,2,3,\ldots$ (i.e. when the frequency of the incident waves corresponds to the natural frequencies of the girder), we find that $|\Delta_1| = |\Delta_2|$. As was mentioned before, $\Delta_1 = \Delta_2$ for $n = 1,3,5,\ldots$ and $\Delta_1 = -\Delta_2$ for $n = 2,4,6,\ldots$, i.e. the two end displacements are 180 degrees out of phase. This observation gives us a better idea about the phase difference between the two amplitudes Δ_1 and Δ_2, as shown, for example, in Figure 10. In some cases, $\Delta_1 = \Delta_2 \simeq 0$ at $\eta = n\pi/\varepsilon$, $n = 1,2,3,5$, as in Figures 5(b), 7, 8 and 9(c) for the second mode, Figure 7(c) for the first mode and Figure 8(c) for the third mode, for example.

5. The peak amplitudes of the displacements Δ_1 and Δ_2 may be relatively high in some cases (e.g. Figures 5 to 9). For the cases studied, these amplitudes are as much as four times greater than they would be if the foundations did not interact with the soil. These peaks occur at frequencies which increase as the parameter ε increases for a constant span. Therefore, the more flexible the girder, the higher the frequency at which the peak occurs. Increasing the span while holding ε constant decreases the frequencies of these peaks. This corresponds to increasing the rigidity of the bridge with respect to that of the soil since $\varepsilon = (\beta_s/\beta_b)(L/R_2)$.

6. When the mass of the foundations increases with respect to that of the girder, the peak values of the Δ_1 and Δ_2 amplitudes increase moderately. This additional increase results from increasing the span, which also decreases the significance of the interaction (e.g. Figures 5 and 8).

7. When the mass of the girder increases with respect to that of the foundation (e.g. Figures 6 and 9), the peak amplitudes of Δ_1 and Δ_2 decrease appreciably. As the span increases, this effect becomes less pronounced.

8. In general, as the span L increases, there is a greater degree of fluctuation in both Δ_1 and Δ_2 amplitudes. For constant L, the fluctuations of Δ_1 and Δ_2 decrease as the angle of incidence θ approaches 90 degrees, since in that case the projected wavelength on the horizontal surface $\lambda_s^* = \lambda_s/\cos\theta$ becomes infinite.

9. When the sizes of the two foundations differ, more complicated interaction phenomena occur (Figures 11 and 12):

(a) When the incident wave first hits the larger foundation (the left one), i.e. when $\theta = 0$ or 45 degrees, this foundation acts as a shield for the right foundation. This shielding effect is most evident in Figures 11(a) and (b) and 12(a), where the smaller foundation moves with nearly the same displacement as the larger one. The additional amplification effects caused by the smaller foundation are negligible in all these cases because of the massiveness of the larger foundation. The shielding effect decreases with an increase of the following parameters:

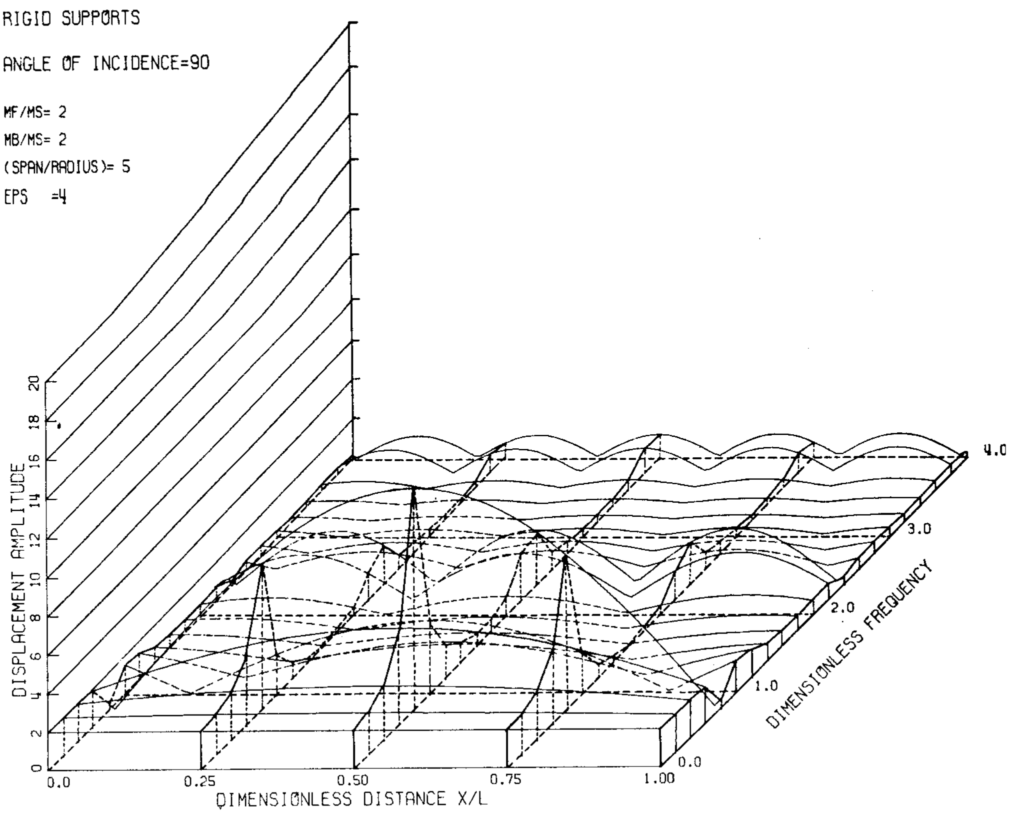

(a)

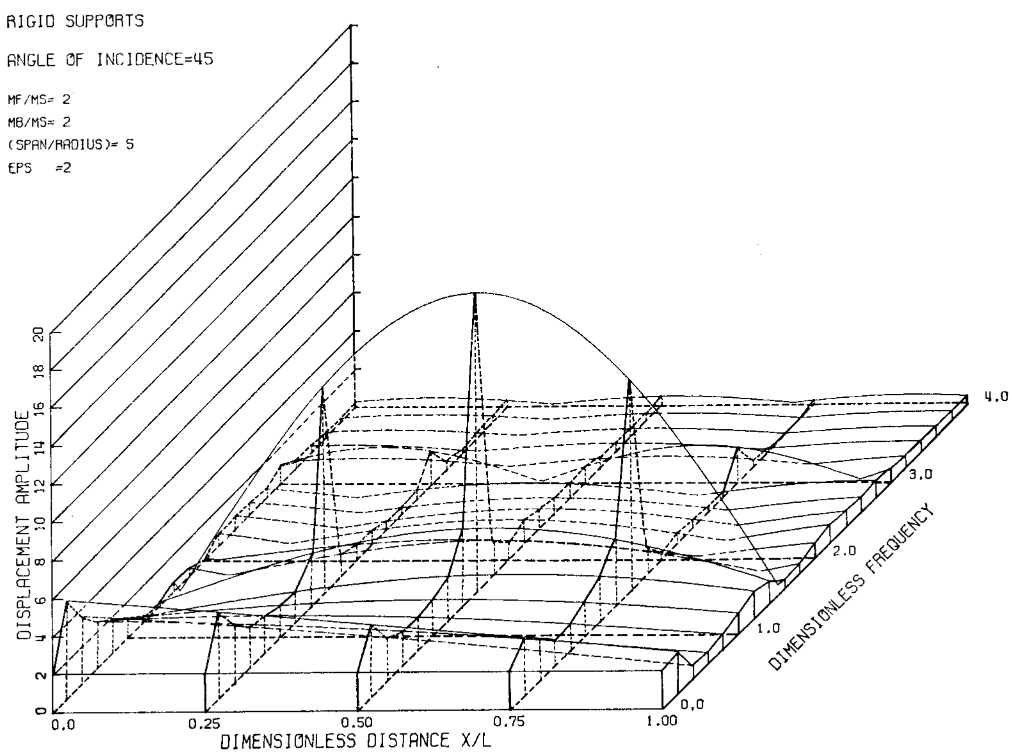

(b)

Figure 10. Displacement amplitude at different points on the girder with (a) the symmetric mode shapes, (b) the first, second and third mode shapes

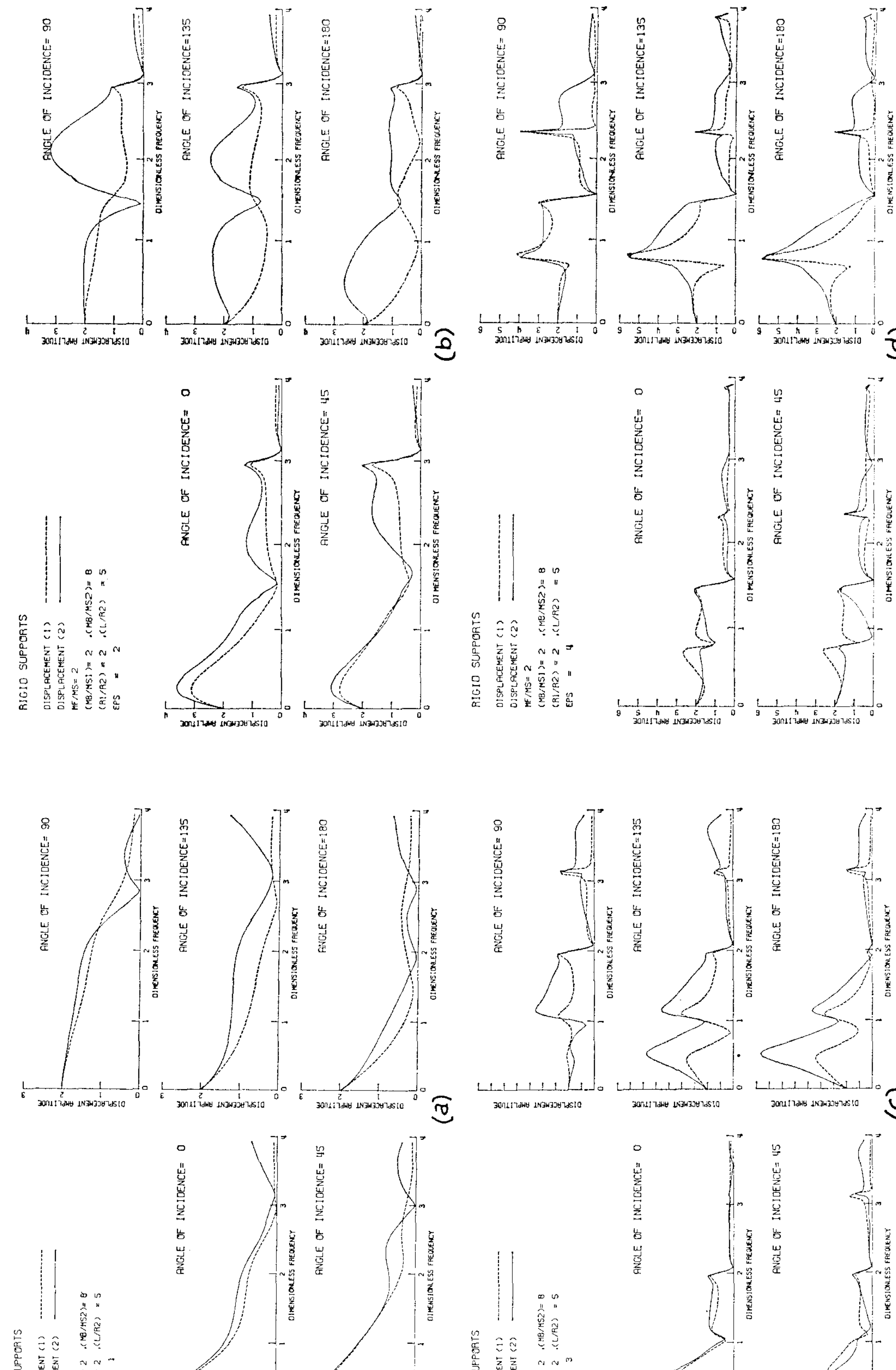

Figure 11. Foundation displacements with MF/MS1 = 2, MF/MS2 = 8, $R_1/R_2 = 2$, $L/R_2 = 5$ and $\varepsilon = 1, 2, 3, 4$

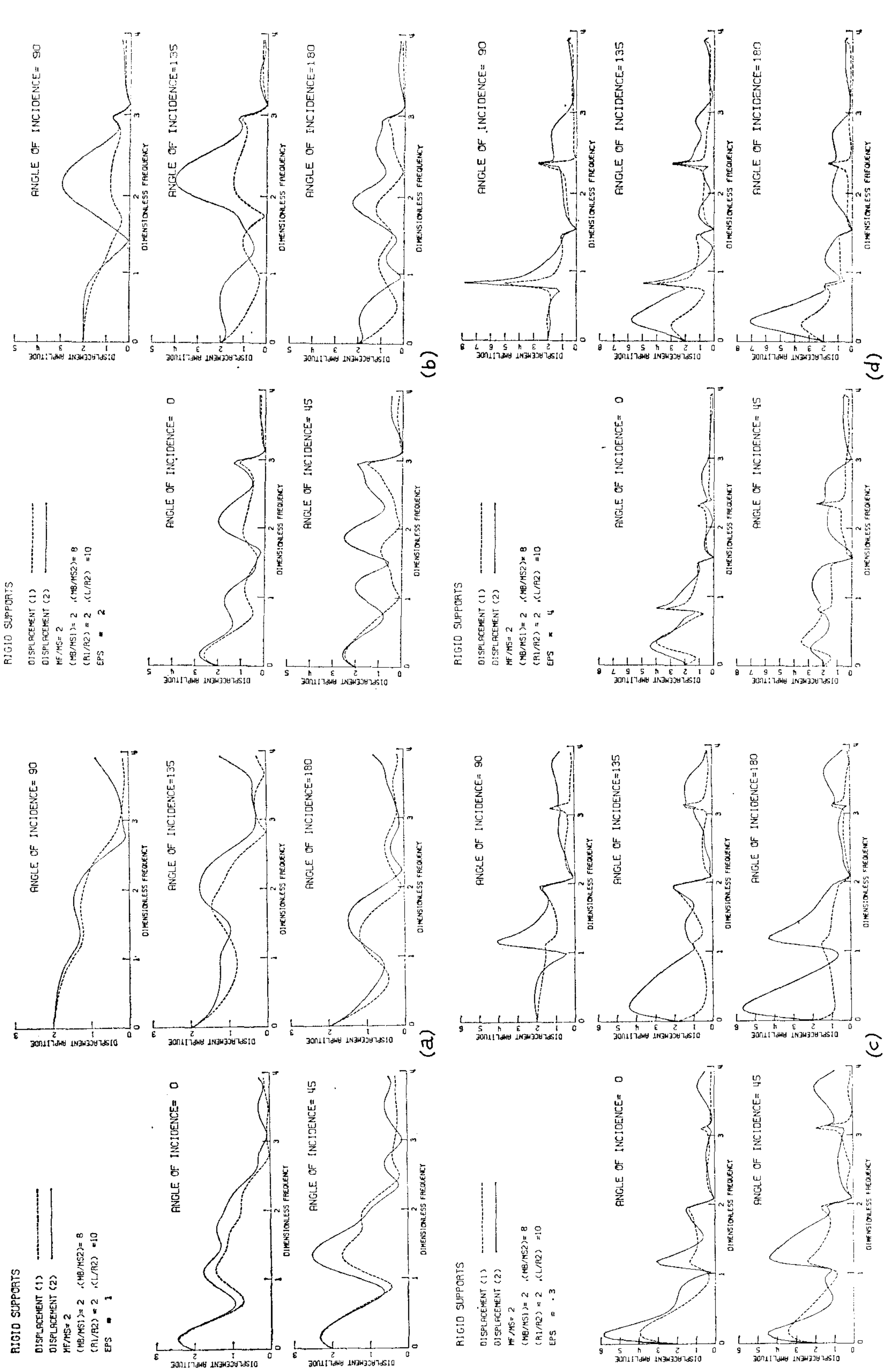

Figure 12. Foundation displacements with MF/MS1 = 2, MF/MS2 = 8, R_1/R_2 = 2, L/R_2 = 10 and ε = 1, 2, 3, 4

1. The flexibility of the girder.
2. The span (Figure 11).
3. The angle of incidence θ.
4. The ratio R_2/R_1 for the same span (Figures 11 and 12).

(b) When the incident wave first hits the smaller foundation (the right one), i.e. when $\theta = 135$ or 180 degrees, the left foundation acts as a barrier which reflects significant wave energy back towards the small foundation while the shielding effect provided by the right foundation is negligible (Figures 11(b) and 12(b)). The overall amplitudes of Δ_1 and Δ_2 are influenced by:

1. The flexibility of the girder.
2. The span and the size of the foundations.
3. The angle of incidence θ.

(c) The peak value of the displacement amplitudes Δ_1 and Δ_2 increases with the increase of the flexibility of the superstructure and the increase of ratio R_1/R_2 [Figures 11(b) and 12(a), (b) and (c)].

(d) For both vertical and non-vertical incident waves, small amplitudes of $|\Delta_1|$ and $|\Delta_2|$ occur at $\eta = n\pi/\varepsilon$, $R_1/R_2 \neq 1$, $n = 1, 3, 5, \ldots$ as shown in Figures 11 and 12. Since $R_1 \neq R_2$, the bridge system is not symmetric now and, in general, we do not expect to find that $|\Delta_1| = |\Delta_2|$ for all θ and $\eta = (n\pi/\varepsilon)(R_1/R_2)$.

RESPONSE OF THE BRIDGE

From the earthquake engineering point of view, one of the more important problems is to find which are the critical sections of a structure and to estimate where the maximum displacements or the maximum stresses may occur. With this in mind, and to illustrate the effects of soil-bridge interaction on the girder of the single-span bridge studied in this paper, we examine in some detail the response of the midpoint and the two quarter points ($x/L = 0{\cdot}25$, $0{\cdot}75$), as shown in the three-dimensional Figure 10.

Using equation (14) for $x = L/2$, we calculate the displacement amplitude $|w(L/2, t)|$ at the midpoint of the span as

$$w\left(\frac{L}{2}, t\right) = \left[\cos\left(\frac{k_b L}{2}\right) - \cot(k_b L)\sin\left(\frac{k_b L}{2}\right)\right]\Delta_1 + \left[\operatorname{cosec}(k_b L)\sin\left(\frac{k_b L}{2}\right)\right]\Delta_2$$

which reduces to

$$\left|w\left(\frac{L}{2}, t\right)\right| = \left|\frac{(\Delta_1 + \Delta_2)}{2}\sec\left(\frac{k_b L}{2}\right)\right| \tag{29}$$

When interaction is neglected, both Δ_1 and Δ_2 would become 1 and $|w(L/2, t)|$ would become infinite at the natural frequencies of the shear beam, i.e. at $k_b L = n\pi$, $n = 1, 3, 5, \ldots$ (since there is a contribution only from the symmetric modes for the midpoint). However, if interaction is not neglected, by using the results from the above analysis the following can be said about the beam response.

1. When $\Delta_1 = \Delta_2 = 0$ at $\eta = n\pi/\varepsilon$; $n = 1, 3, 5, \ldots$; $R_1 = R_2$; i.e. in the case of vertical SH-waves where $\theta = 90$ degrees, the response given by (29) remains finite and is characterized by relatively small peaks, as shown, for example, in Figure 13. It can also be seen in this figure that when $\theta \neq 90$ degrees the peaks, in general, are much larger and the effect of small Δ_1 and Δ_2 is less pronounced.
2. When Δ_1 and Δ_2 have considerable amplitudes at $\eta = n\pi/\varepsilon$, $n = 1, 3, 5, \ldots$, and in the case of non-vertically incident SH-waves, the amplitude of the beam response is large at $\eta = n\pi/\varepsilon$, i.e. at the fundamental resonant frequencies of the beam. It should be noted that the sharp peaks in Figure 13 have been plotted only up to the amplitude equal to 40 to preserve the detail and resolution of the neighbouring smaller amplitudes.

Other important characteristics of the results which can be shown in figures similar to Figure 13 can be summarized as follows: In general, the peak values of $|w(L/2, t)|$ increase with ε, when $\theta = 90$ degrees, i.e. for higher flexibility of the structure with respect to that of the soil and for the MB/MS fixed. The peak response amplitudes decrease for the higher modes and for the same ε. Increasing the foundation mass

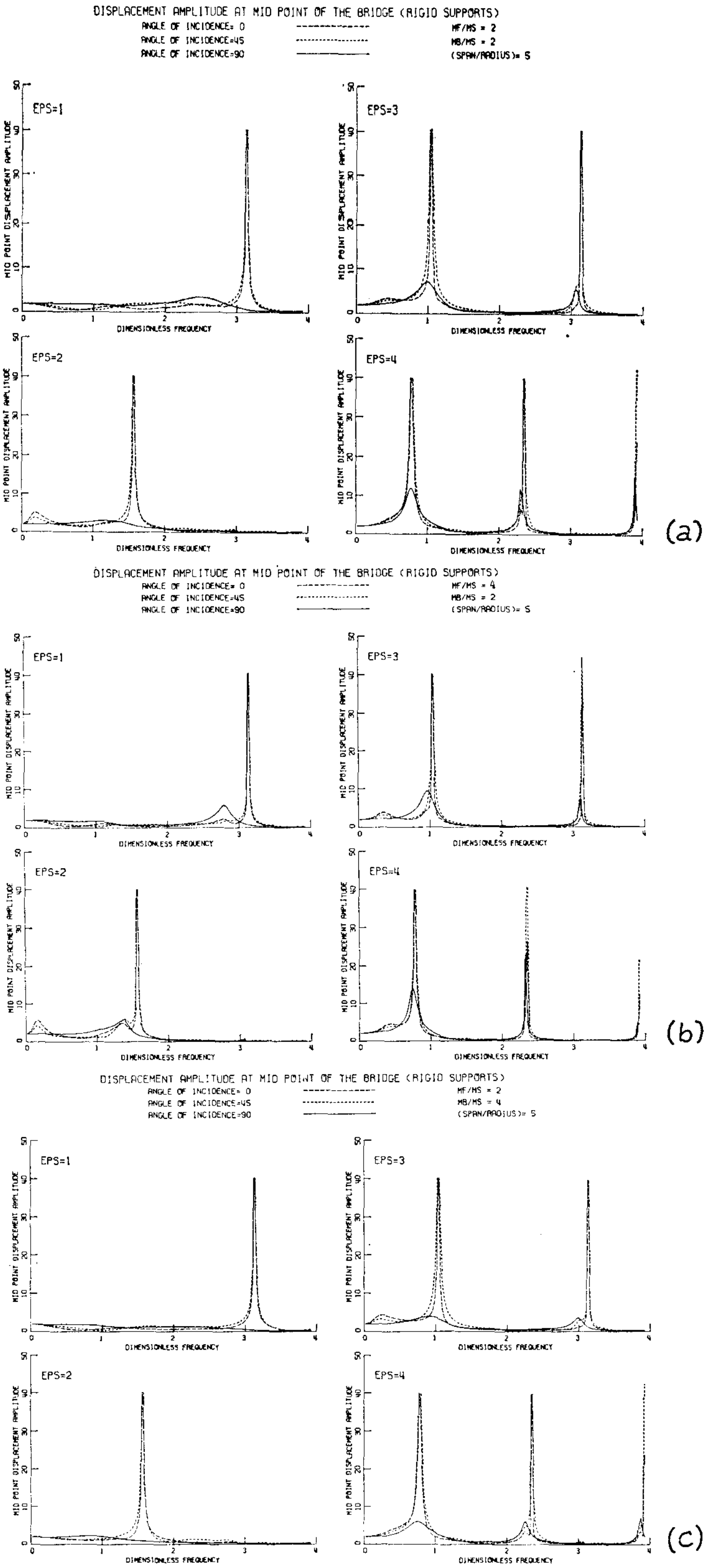

Figure 13. Displacement amplitude at the midpoint of the girder with (a) MF/MS = 2, MB/MS = 2, $L/R_2 = 5$, (b) MF/MS = 4, MB/MS = 2, $L/R_2 = 5$, (c) MF/MS = 2, MB/MS = 4, $L/R_2 = 5$

[larger (MF/MS)] leads to more effective coupling of the bridge to the soil and thus less radiative damping, while increasing the mass of the girder [larger (MB/MS)] leads to higher radiative damping when L is constant. The increase of span L for a fixed value of ($\beta_b/\beta_s = L/\varepsilon R_2$), which is equivalent to increasing the rigidity of the girder with respect to that of the soil, also leads to more radiative damping.

CONCLUSIONS

A key step in the evaluation of the soil-structure interaction effects on the earthquake response of a structure is in the computation of the force-displacement relationships for the foundation. Several such relationships,[2,5,8,9] expressed in terms of impedance or compliance functions, are available in the literature.

Having obtained the impedance function for particular two-dimensional abutment conditions, represented by rigid foundations with semicircular cross-sections, and having defined the input motion in terms of plane SH-waves, the calculation of the response of the bridge girder depends on the stiffness, mass and damping characteristics of the bridge relative to that of the soil. For some input frequencies the amplitude of the foundation response has been found to be significantly larger than the free field surface displacement amplitude which could be obtained for the same excitation in the absence of a bridge or its abutments.

The excitation of different modes of vibration of the two-dimensional bridge girder is related to the nature of the foundation movement for different angles of incident SH-waves and, in particular, depends on the relative phase of motion for two bridge abutments. When two abutments move in phase, there is a tendency to excite symmetric modes of girder vibration; while when they are moving out of phase, the antisymmetric modes are excited more effectively. The simplest type of the two-dimensional soil-bridge interaction occurs for the vertical incidence of SH-waves and for the symmetric bridge and its abutments. In that case, for the frequencies that correspond to the symmetric modes of girder vibration, the two abutments do not move and the efficiency of radiation damping, which results from the wave scattering from the two foundations, is maximum. In all other cases, when the angle of incident waves is not vertical, or when the bridge girder is not symmetric and/or when the abutments are different, this simplicity is lost and the efficiency of radiative damping is significantly reduced. In general, when the angle of incident SH-waves is not vertical, a large response of the bridge is obtained at the fixed base natural frequencies of the bridge.

When the bridge and its abutments are symmetric, the torsional motion of the whole bridge does not seem to be excited appreciably, at least not for the mass ratios and the geometries studied in this paper. However, this tendency is completely reversed when the bridge abutments are not the same (i.e. $R_1 \neq R_2$ and/or MS1 $\neq$ MS2). Non-symmetry of mass distributions enhances the overall torsional response, especially for horizontally incident SH-waves. Other related phenomena, such as shielding, amplification by the wave scattered from the other foundation and the influence of the standing wave pattern on the excitation of two bridge abutments, are all accentuated and made more complex by the non-symmetry of the two abutments.

ACKNOWLEDGEMENTS

We are grateful to H. L. Wong, who gave us his computer program for calculation of compliances and driving forces, and for his kind help and many useful suggestions. We also are indebted to J. E. Luco for critical reading of the manuscript and to one of the referees whose critical comments contributed significantly to the final version of this paper.

This research has been supported by grants from the National Science Foundation and by a contract from the United States Geological Survey.

REFERENCES

1. G. W. Housner, 'Interaction of building and ground during an earthquake', *Bull. Seism. Soc. Am.* **47**, 179–186 (1957).
2. J. E. Luco, 'Dynamic interaction of a shear wall with the soil', *J. Eng. Mech. Div., ASCE*, **95**, 333–345 (1969).
3. M. D. Trifunac, 'Interaction of a shear wall with the soil for incident plane SH-waves', *Bull. Seism. Soc. Am.* **62**, 63–83 (1972).
4. H. B. Seed and I. M. Idriss, 'Soil-structure interaction of massive embedded structures during earthquakes', *Proc. 5th Wld Conf. Earthq. Engng*, Rome, Italy, 1973.

5. J. E. Luco and L. A. Contesse, 'Dynamic structure-soil-structure interaction', *Bull. Seism. Soc. Am.* **63**, 1284–1303 (1973).
6. S. Okamoto, *Introduction to Earthquake Engineering*, Wiley, New York, 1973, pp. 301–374.
7. R. L. Wiegel, *Earthquake Engineering*, Prentice-Hall, Englewood Cliffs, N.J., 1970.
8. J. E. Luco, H. L. Wong and M. D. Trifunac, 'A note on the dynamic response of rigid embedded foundations', *Int. J. Earthq. Engng Struct. Dyn.* **4**, 119–127 (1975).
9. H. L. Wong and M. D. Trifunac, 'Two-dimensional, antiplane, building-soil-building interaction for two or more buildings and for incident plane SH-waves', *Bull. Seism. Soc. Am.* **65**, 1863–1885 (1975).
10. S. A. Thau, 'Radiation and scattering from a rigid inclusion in an elastic medium', *J. Appl. Mech.* **34**, 509–511 (1967).